Development 138, 619-629 (2011) doi:10.1242/dev.054536

Rumba and Haus3 are essential factors for the maintenance of hematopoietic stem/progenitor cells during zebrafish hematopoiesis

Linsen Du[1,2,*], Jin Xu[1,*], Xiuling Li[1], Ning Ma[3], Yanmei Liu[4,5], Jinrong Peng[6], Motomi Osato[2], Wenqing Zhang[3] and Zilong Wen[1,†]

SUMMARY

The hallmark of vertebrate definitive hematopoiesis is the establishment of the hematopoietic stem/progenitor cell (HSPC) pool during embryogenesis. This process involves a defined ontogenic switching of HSPCs in successive hematopoietic compartments and is evolutionarily conserved from teleost fish to human. In zebrafish, HSPCs originate from the ventral wall of the dorsal aorta (VDA), from which they subsequently mobilize to an intermediate hematopoietic site known as the caudal hematopoietic tissue (CHT) and finally colonize the kidney for adult hematopoiesis. Despite substantial understanding of the ontogeny of HSPCs, the molecular basis governing migration, colonization and maintenance of HSPCs remains to be explored fully. Here, we report the isolation and characterization of two zebrafish mutants, *rumba*^{hkz1} and *samba*^{hkz2}, that are defective in generating definitive hematopoiesis. We find that HSPC initiation in the VDA and subsequent homing to the CHT are not affected in these two mutants. However, the further development of HSPCs in the CHT is compromised in both mutants. Positional cloning reveals that Rumba is a novel nuclear C2H2 zinc-finger factor with unknown function and *samba* encodes an evolutionarily conserved protein that is homologous to human augmin complex subunit 3 (HAUS3). Furthermore, we show that these two factors independently regulate cell cycle progression of HSPCs and are cell autonomously required for HPSC development in the CHT. Our study identifies Rumba and Haus3 as two essential regulators of HSPC maintenance during zebrafish fetal hematopoiesis.

KEY WORDS: Zebrafish, Definitive hematopoiesis, Hematopoietic stem/progenitor cells, Ontogeny, Ventral wall of dorsal aorta, Caudal hematopoietic tissue

INTRODUCTION

Vertebrate hematopoiesis is a complex biological process that occurs in two successive waves. The first, or primitive, wave of hematopoiesis produces mainly embryonic red blood cells and some myeloid cells (Moore and Metcalfe, 1970). This transitory wave is rapidly replaced by the definitive wave of hematopoiesis, which can generate all the blood lineages during fetal life and adulthood. This unique feature of definitive hematopoiesis relies on the definitive hematopoietic stem/progenitor cells (HSPCs), which are capable of self-renewal and differentiation into all hematopoietic lineages (Morrison et al., 1995; Weissman, 2000). In mice, the original pool of HSPCs is established during embryogenesis in a complex developmental process that involves several anatomical sites. The intraembryonic region known as aorta-gonad-mesonephros (AGM) has been widely viewed as the initial site for HSPC production (Muller et al., 1994; Cumano et al., 1996; Medvinsky and Dzierzak, 1996), although the yolk sac and placenta also contribute to this HSPC pool (Gekas et al., 2005; Ottersbach and Dzierzak, 2005; Samokhvalov et al., 2007). The AGM-derived HSPCs then travel to other intermediate hematopoietic sites, such as the fetal liver and possibly the placenta, where they undergo rapid expansion and further differentiation (Mikkola and Orkin, 2006). During postnatal life, HSPCs colonize the bone marrow, in which they undergo differentiation and self-renewal to replenish the loss of peripheral blood cells and maintain the HSPC pool throughout the lifetime of the organism (Cheshier et al., 1999). The ontogeny of definitive HSPCs has been well studied by morphological analysis and functional assays over the years. However, the molecular programs that specify this process are still incompletely defined, partly owing to the fact that most of the genes and pathways involved in HSPC development were identified using reverse genetic approaches in mice. Thus, investigation in other model systems that allow an unbiased phenotype-driven approach is expected to complement our current knowledge from mammals (de Jong and Zon, 2005; Lieschke and Currie, 2007; Trede et al., 2008).

Owing to its unique embryological and genetic advantages, zebrafish has been recognized as a pre-eminent vertebrate model organism for the study of hematopoiesis (Bahary and Zon, 1998; Amatruda and Zon, 1999). Similar to other higher vertebrates, zebrafish hematopoiesis consists of two successive waves of development and produces multilineage hematopoietic cells that are analogous to their mammalian counterparts (Traver et al., 2003; Davidson and Zon, 2004). Definitive hematopoiesis in zebrafish begins in the ventral wall of the dorsal aorta (VDA) at ~28 hours post-fertilization (hpf) as demonstrated by HSPC-associated gene expression and lineage tracing data (Thompson et al., 1998; Willett

[1]State Key Laboratory of Molecular Neuroscience, Department of Biochemistry, Hong Kong University of Science and Technology, Clear Water Bay, Kowloon, Hong Kong, P.R. China. [2]Cancer Science Institute of Singapore, National University of Singapore, Centre for Life Sciences, #02-07, 28 Medical Drive, Singapore 117456. [3]Department of Cell Biology, Southern Medical University, Guangzhou 510515, P.R. China. [4]Max Planck Institute of Molecular Cell Biology and Genetics, Dresden 01307, Germany. [5]Laboratory of Experimental Diabetology, Carl Gustav Carus Medical School, Dresden University of Technology, Dresden 01307, Germany. [6]College of Animal Sciences, Zhejiang University, 268 Kai Xuan Road, Hangzhou, 310029, P.R. China.

*These authors contributed equally to this work
†Author for correspondence (zilong@ust.hk)

Accepted 25 November 2010

et al., 2001; Kalev-Zylinska et al., 2002; Burns et al., 2002; Murayama et al., 2006; Zhang and Rodaway, 2007; Jin and Wen, 2007; Kissa et al., 2008), suggesting that the VDA is analogous to the mammalian AGM region. Notch, Hedgehog and Prostaglandin-Wnt pathways, as well as biomechanical stimulation by blood flow, have been shown to be crucial for the generation of definitive HSPCs in the VDA region (Gering and Patient, 2005; Burns et al., 2005; North et al., 2007; North et al., 2009; Goessling et al., 2009; Burns et al., 2009). By 2 days post-fertilization (dpf), the majority of these VDA-derived HSPCs have mobilized to the caudal hematopoietic tissue (CHT), an intermediate hematopoietic site analogous to the mouse fetal liver, to support the expansion and differentiation of VDA-derived HSPCs (Murayama et al., 2006; Jin et al., 2007; Kissa et al., 2008). Those HSPCs ultimately colonize the adult hematopoietic organ-kidney (by 5 dpf) signifying the establishment of long-lasting definitive hematopoiesis (Bertrand et al., 2008). Despite these recent progresses in elucidating the developmental path of HSPCs, little is known about the molecular basis of migration, colonization and maintenance of HSPCs. To uncover such mechanisms, our laboratory has carried out forward genetic screens in zebrafish in search of genes involved in HSPC development during definitive hematopoiesis.

Here, we report the isolation and characterization of two definitive hematopoiesis-deficient zebrafish mutants, *rumba*^{hkz1} and *samba*^{hkz2}, from our N-ethyl-N-nitrosourea (ENU) mutant collection. Phenotype analysis showed that both *rumba*^{hkz1} and *samba*^{hkz2} mutants carried out primitive hematopoiesis normally but had severe defects in the generation of definitive erythroid, myeloid and lymphoid cells. A closer examination of these two mutants revealed that definitive HSPCs were properly specified in the VDA region and could subsequently migrate to the CHT, but their further development in the CHT could not be sustained**.** Positional cloning revealed that *rumba*^{hkz1} and *samba*^{hkz2} mutations were in genes encoding a novel C2H2 zinc-finger factor and an evolutionarily conserved protein homologous to the human augmin complex subunit 3 (HAUS3), respectively. Transplantation analysis further demonstrated that both of these proteins, called Rumba and Haus3, were cell autonomously required for maintaining HSPCs in the CHT during fetal hematopoiesis.

MATERIALS AND METHODS

Fish lines and ethylnitrosourea (ENU) mutagenesis

Zebrafish strain AB was used as the wild-type strain for normal crossing and WIK was used as the mapping strain. The Tg(*cd41:*eGFP) transgenic line used in this study was described by Lin et al. (Lin et al., 2005). ENU (Sigma) mutagenesis was carried out as described (Solnica-Krezel et al., 1994; Mullins et al., 1994).

Single color whole-mount in situ hybridization (WISH)

Antisense RNA probes were labeled with digoxigenin (DIG) using the DIG-RNA Labeling Kit (Roche). WISH was performed as described previously with NBT/BCIP (Sigma) as substrate (Westerfield, 2000). Images were taken using a Nikon AZ100 microscope.

Double staining of *cmyb* RNA and phospho histone 3 protein (pH3)

To detect *cmyb* RNA and mitosis marker pH3 simultaneously, embryos were first hybridized with the DIG-labeled antisense *cmyb* RNA probe as described for single color WISH. After washing and blocking, the embryos were incubated at 4°C overnight with a peroxidase (POD)-conjugated anti-DIG antibody (1:500; Roche) and stained with Alexa Fluor 488-conjugated tyramide as substrate (PerkinElmer) according to the manufacturer's instructions. After three 20-minute washes with PBST (0.1% Tween in PBS) at room temperature (RT), the embryos were soaked in PBDT [PBS with 0.1% Triton X-100, 1% bovine serum albumen (BSA) and 1% DMSO] plus 2% lamb serum for 1 hour at RT and then incubated with primary antibody anti-pH3 (ser10) (1:400; Upstate) at 4°C overnight. After removing the primary antibody, the embryos were washed with PBDT and finally incubated with Alexa Fluor 488-labeled goat anti-rabbit IgG antibody (1:400; Molecular probes). Images were taken using a Zeiss LSM 510 confocal microscope.

BrdU labeling and triple staining

BrdU labeling was performed as described (Wallace et al., 2005). In brief, BrdU (30 mM; Sigma) was injected peritoneally into 3 dpf *rumba*$^{hkz1-/-}$/Tg(*cd41:*eGFP) embryos or siblings. The injected embryos were incubated for 2 hours and fixed in 4% paraformaldehyde (PFA). The fixed embryos were dehydrated with methanol and kept at –20°C overnight. After rehydration, the embryos were treated with Proteinase K (10 μg/ml) for 15 minutes at RT and re-fixed in 4% PFA for 30 minutes. Following washing with PBST, the embryos were incubated with 2 N HCl for 1 hour at RT, rinsed with PBST and then blocked in 1% BSA for 1 hour. Finally, the embryos were stained with anti-BrdU (Roche), anti-pH3 (Upstate) and anti-GFP (Abcam) antibodies according to the manufacturer's protocol. Alexa Fluor 555-conjugated anti-mouse, Alexa Fluor 647-conjugated anti-rabbit, and Alexa Fluor 488-conjugated anti-goat secondary antibodies (Invitrogen) were used for triple staining.

Apoptotic assay by Acridine Orange staining and TUNEL assay

In brief, embryos were dechorionated and placed in 5 μg/ml Acridine Orange (AO; Sigma) in egg water. After 30-60 minutes, the embryos were washed with egg water and visualized using a fluorescent microscope (Furutani-Seiki et al., 1996). For the TUNEL (terminal deoxynucleotidyl transferase dUTP nick end labeling) assay, PFA-fixed embryos were permeabilized by treatment with a proteinase K (10 μg/ml) and acetone:ethanol (1:2) mixture at –20°C and then stained using the In Situ Cell Death Detection Kit TMR red (Roche) according to the manufacturer's instructions.

Vessel injection

Approximately 1 nl 5% tetramethylrhodamine dextran (10,000 MW, Invitrogen, D1868) was injected intravenously into the circulation of 4 dpf embryos.

Positional cloning

Positional cloning was performed as described previously (Bahary et al., 2004). The *rumba*^{hkz1} mutation was first mapped to linkage 16 between the simple sequence length polymorphism markers (SSLPs) z63822 and z62948. Two closer markers, Z63822 and J95743, were used for analyzing 1717 *ramba*$^{hkz1-/-}$ embryos for recombinant events. The region containing the *rumba*^{hkz1} mutation was further narrowed down to a 184 kb region by 1 North (O82105) and 4 South (J95743, R101392, L131863 and L25805) SSLP markers. The *rumba*^{hkz1} mutation was revealed by sequencing the genomic sequence of the four candidate genes within this region. The primers used for positional cloning of the *rumba*^{hkz1} mutation were: Z62948 (5′-CCGACACACACCTACCCTCT-3′, 5′-TGCGCTTGTATAGAGGCATG-3′); J95743 (5′-CCGGCCCTCCTGGTGTCCTACAT-3′, 5′-GTTTGCCGCTCCGCCATCAC-3′); R101392 (5′-CTGCTGAAGAACAGGATGGA-3′, 5′-TGAGCTCTGCATTTGCATTC-3′); L131863 (5′-TCGCAAGTGGAAAGATCAAA-3′, 5′-TCCATCCCTTTCTCGCATAG-3′); L25805 (5′-ATCACTGGGGTCGTCATTGGA-3′, 5′-CTCTGTGGAGCCATTCTGAGCAG-3′); Z63822 (5′-TGTGGAGGTAGTTTTTGAGGG-3′, 5′-TCCCCAACAATCTCCAACTC-3′); O82105 (5′-GGGCAAGTGTTTTTGCTCAT-3′, 5′-TGTTAGAATCTCATTTAGAACAAAGCA-3′). The primers used for genotyping analysis were: 5′-CTGTCTGTCTTTGTTTGCAGAC-3′, 5′-CGCAGAACTCGCAGGTGAAG-3′.

Bulk segregate analysis showed the *samba*^{hkz2} mutation to be linked with two SSLP markers, z4706 and z1059, on chromosome 7. In fine mapping, two closer SSLP markers, zK183N2-118 and z4706, were used for analyzing 1910 *samba*^{hkz2} embryos for recombinant events. Two markers CR318672_119281 and CR318603_55485 further positioned the *samba*^{hkz2} mutation to a region covered by three overlapping bacterial artificial

chromosomes (BACs), CR318672, CR376795, and CR318603, on contig 676. Finally, the *samba*^{hkz2} mutation was identified by sequencing the genomic sequence of candidate genes. The primers used for positional cloning of the *samba*^{hkz2} were: z4706 (5′-TGCATATAGGCACCTCCA-3′, 5′-TTTCCCCATCAACAAAGCTC-3′); z1059 (5′-CACAGCATCA-CGCTCTCACT-3′, 5′-TATACCGTGGAAATTTCGGG-3′); zK183N2_118 (5′-TGCAAATACAATGCATACCG-3′, 5′-TGCGTACAAGACGGTAA-CAAA-3′); CR318672_119281 (5′-GCATTCAGATTCTGGGGTGT-3′, 5′-CGGATGAACCCATCAATCTC-3′); CR318603_55485 (5′-CCAG-GAGAGCTCGCACTAAG-3′, 5′-GACCATTGGAAAAGGGCTTC-3′). The primers used for genotyping analysis were: 5′-GAGAACTCAT-TTGTGTCACCA-3′, 5′-TTTACTGCATTTATCCCTC-3′.

Polyclonal anti-Rumba and anti-αE1-globin antibody production

Glutathione-s-transferase (GST)-Rumba (amino acids 170-300) and GST-αE1-globin (full-length) fusion proteins were used as antigens for rabbit immunization. Rabbit blood sera were collected and purified as described previously (Jin et al., 2006).

Intracellular localization of Rumba and Haus3

To examine the subcellular localization of the Rumba protein, *rumba* was ectopically expressed in fish embryos by plasmid injection and detected with a rabbit anti-Rumba antibody. Finally, the embryos were incubated with mounting medium containing DAPI and observed using a Zeiss LSM 510 confocal microscope.

For Haus3 protein cellular localization, Cos-7 cells were grown on coverslips in a 6-well dish and transfected with *pcDNA3.1/nV5-haus3*-α/β (*haus3* gene fused with a V5 Tag at the N terminus) using lipofectomine (Invitrogen). After a brief wash with ice-cold PBS-CM (PBS with 1 mM $CaCl_2$ and 1 mM $MgCl_2$), the transfected cells were fixed in 3% PFA in PBS-CM for 20 minutes, washed twice with PBS-CM followed by two washes in 0.3% NH_4Cl in PBS-CM and, finally, PBS-CM. The cells were then permeabilized in PBS-CM containing 0.1% Triton X-100 for 15 minutes and incubated with monoclonal anti-V5 antibody (1:200; Invitrogen) in FDB (PBS-CM with 5% goat serum, 2% fetal bovine serum and 2% BSA). After six rinses with 0.1% Triton X-100 in PBS-CM, the cells were incubated with Alexa Fluor 488-conjugated anti-mouse IgG antibody (1:400; Molecular Probes) and washed with 0.1% Triton X-100 in PBS-CM. The coverslips were mounted with mounting medium containing DAPI for fluorescence (Vector Laboratories).

Plasmid construction and rescue experiment

In order to obtain the full-length cDNA, rapid amplification of cDNA ends (RACE) was performed according to the manual of the FirstChoice RLM-RACE Kit (AM1700, Ambion). A 3 kb cDNA fragment including the entire coding region of *rumba* (accession number GU232734) was amplified with primers *Eco*RI-*rumba*-1f (5′-ccggaattcAATCACGGTGCGTTTTGTTGAG-3′) and *Xba*I-*rumba*-3102r-c (5′-ctagtctagaTCACACAGTCTCCTCT-AAGATGA-3′). The full-length *haus3*-β (*zgc:153228*-β) cDNA (accession number GU269274) was amplified using the following primers: 5′-ATCACCTTCAACGATAAACTTT-3′, 5′-GAGATAACAAATATTTATT-AAC-3′). The *haus3*-α (*zgc:153228*-α) cDNA (accession number BC124280 or BK006950) was obtained from I.M.A.G.E. clone (Open Biosystems). All the amplified fragments were cloned into a pCS2$^+$ vector and linearized as templates for generating sense RNA in rescue experiments.

The capped RNA was in vitro transcribed and polyadenylated using the mMessage mMachine High-yield Capped RNA Transcription Kit and the Poly(A) Tailing Kit (Ambion). Approximately 200 pg in vitro transcribed *rumba* RNA and 300 pg *haus3* RNA was injected per embryo at the one-cell stage.

To check the stability of injected RNA, total RNA was extracted from embryos with the RNeasy Mini Kit (QIAgen). Reverse transcription was performed with superscript III reverse transcriptase (Invitrogen). The injected RNA was distinguished from the endogenous RNA by SV40 polyA primers (Sv40-F: TGAGTTTGGACAAACCACAAC; Sv40-R: CCCCCTGAACCTGAAACATA).

For WISH analysis, amplified *rumba* and *haus3*-β fragments were cloned into a pGEM-T Easy vector (Promega) in order to generate antisense RNA probes.

Transplantation experiment

Embryonic transplantation was performed at ~3 hpf as described previously (Westerfield, 2000; Liu et al., 2007). Tg(*cd41*:eGFP) transgenic embryos (wild type or mutants) were used as donors, and a similar number of donor cells was placed into either homozygous mutants or their siblings. The contribution of donor cells in the host was determined by double fluorescence antibody staining of GFP and αE1-globin. Host embryos were fixed at 5 dpf with 4% PFA at RT for 2 hours. After washing, embryos were blocked in PBDT plus 2% lamb serum for 1 hour at RT. The embryos were then incubated with polyclonal goat anti-GFP antibody (1:400; Abcam) at 4°C overnight. After removing the primary antibody, the embryos were washed in PBDT and visualized with the secondary antibody Alexa Fluor 488-conjugated donkey anti-goat IgG (1:400; Molecular Probes). To detect the αE1-globin protein, embryos were washed with PBDT and incubated with rabbit polyclonal raised against zebrafish αE1-globin (1:200) at 4°C overnight. Finally, embryos were washed and signal was visualized using the Alexa Fluor 633-conjugated donkey anti-rabbit IgG antibody (1:400; Molecular Probes).

Living cell cycle analysis

Embryonic cell suspensions from Tg(*cd41*:eGFP) transgenic larvae were prepared as previously described (Liu et al., 2007). Approximately 25 embryos were disaggregated in cold 0.9×PBS with 5% FBS (Hyclone, Logan, UT, USA). The cell suspensions were passed through a 70 μm pore filter and spun at 800 ***g*** for 5 minutes. The pellets were resuspended in 1 ml cell dissociation buffer-free Hanks (Gibco, Carlsbad, CA, USA) and incubated at 37°C for 20 minutes. After the addition of 1 ml washing buffer (Hanks buffered saline solution containing 20% calf serum, 5 mM $CaCl_2$ and 50 μg/ml DNase), the cell suspensions were spun at 800 ***g*** for 5 minutes and resuspended in PBS. After passing through a 40 μm pore filter, the cells (10^6 per ml) were analyzed using a FACS Aria II flow cytometer (Becton Dickinson).

RESULTS

rumba^{hkz1} and *samba*^{hkz2} are definitive hematopoiesis-defective mutants

To gain new insight into the regulation of definitive hematopoiesis, we carried out a forward genetic screen in search of ENU-induced zebrafish mutants with defects in thymic *recombination activating gene 1* (*rag1*) expression. Rag1 is known to catalyze the rearrangement of immunoglobulin genes in immature B lymphocytes and of T cell receptor genes in immature T lymphocytes, respectively (Willett et al., 1997). It is also essential for the development of lymphoid, a lineage derived exclusively from definitive hematopoiesis. Using *rag1* expression as the primary readout, a collection of mutants that had relatively normal morphology and intact angiogenesis but specific defects in the generation of definitive hematopoiesis was obtained. Among them, *rumba*^{hkz1} and *samba*^{hkz2} were two mutant lines with similar phenotypes. Both homozygous *rumba*$^{hkz1-/-}$ and *samba*$^{hkz2-/-}$ mutants were indistinguishable from their siblings at early stages and had an intact vascular system (see Fig. S1 in the supplementary material). However, *rag1* expression was hardly detected in both mutants (Fig. 1A-B′). Their circulation began to slow down gradually after 5 dpf and, eventually, both died at ~7-14 dpf. Consistent with the observation of normal morphology and blood circulation in early stage mutants, primitive hematopoiesis was indeed unaffected in *rumba*$^{hkz1-/-}$ and *samba*$^{hkz2-/-}$ mutants as shown by the normal expression of erythroid *ae1-globin* (*hbae1* – Zebrafish Information Network) gene (Brownlie et al., 2003) and myeloid *mpo* gene (*mpx* – Zebrafish Information Network) (Bennett et al., 2001) (Fig. 1C-F′). These data indicate that, despite a lack of thymic *rag1* expression, both *rumba*^{hkz1} and *samba*^{hkz2} mutants can initiate primitive hematopoiesis normally.

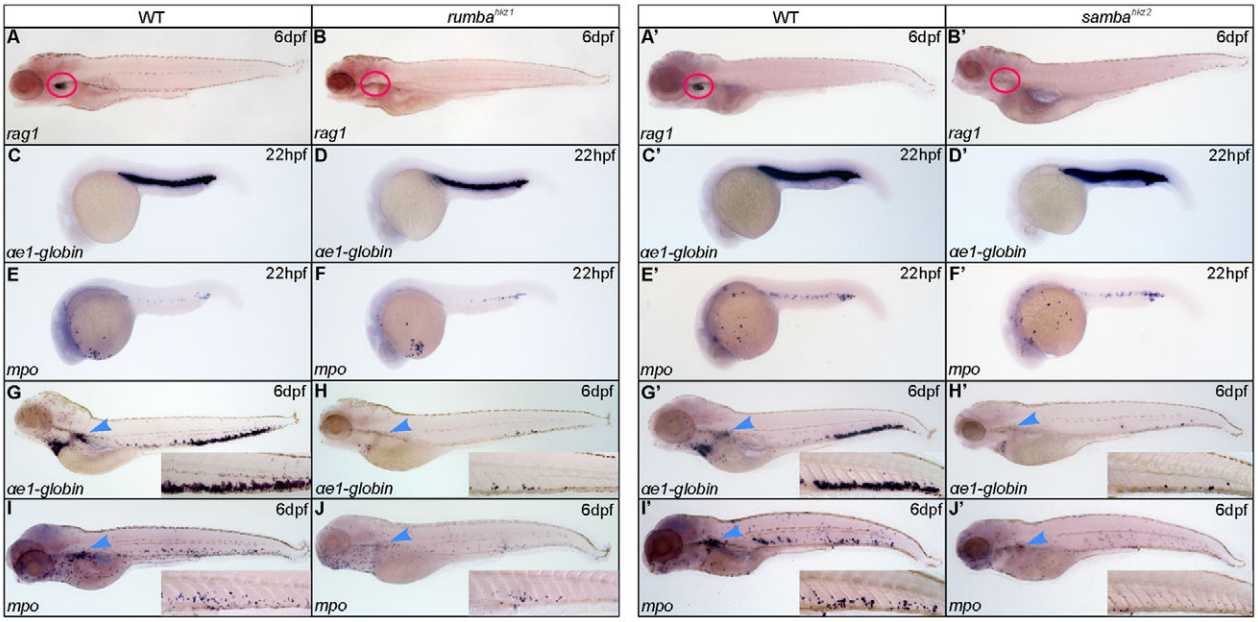

Fig. 1. *rumba*^{hkz1} and *samba*^{hkz2} are defective in definitive hematopoiesis. (**A-B′**) WISH of *rag1* expression in 6 dpf wild-type (WT) zebrafish siblings (A,A′) and *rumba*$^{hkz1-/-}$ (B) and *samba*$^{hkz2-/-}$ mutants (B′). The red circles indicate the position of the thymus. (**C-F′**) WISH of α*e1-globin* (C-D′) and *mpo* (E-F′) in 22 hpf wild-type siblings (C,C′,E,E′) and *rumba*$^{hkz1-/-}$ (D,F), and *samba*$^{hkz2-/-}$ mutants (D′,F′). (**G-J′**) WISH of α*e1-globin* (G-H′) and *mpo* (I-J, I′-J′) in 6 dpf wild-type siblings (G,G′,I,I′) and *rumba*$^{hkz1-/-}$ (H,J) and *samba*$^{hkz2-/-}$ mutants (H′,J′). Insets in G-J′ show enlarged details of the CHT region. The blue arrowheads indicate the position of the kidney.

The lack of thymic *rag1* expression indicates defects in T lymphocytes and prompted us to test whether other hematopoietic lineages, such as erythroid and myeloid cells, of definitive origin were also affected in these two mutants. We therefore examined the transcription of *ae1-globin* and *mpo* in 6 dpf *rumba*$^{hkz1-/-}$ and *samba*$^{hkz2-/-}$ larvae when definitive erythroid and myeloid lineages are evident in the CHT and kidney (Jin et al., 2009). In wild-type embryos, definitive erythroid precursors were found mainly in the CHT and the kidney as shown by the robust *ae1-globin* expression (Fig. 1G,G′). Similarly, *mpo*-expressing definitive myeloid cells predominantly resided in the kidney and scattered across the CHT region (Fig. 1I,I′). However, these expression patterns of both *ae1-globin* and *mpo* were almost wiped out in the 6 dpf *rumba*$^{hkz1-/-}$ and *samba*$^{hkz2-/-}$ mutant larvae (Fig. 1H,H′,J,J′). Thus, in addition to the defective lymphoid lineage development, definitive erythroid and myeloid lineages were also severely impaired in *rumba*$^{hkz1-/-}$ and *samba*$^{hkz2-/-}$ mutants, strongly suggesting that both *rumba*^{hkz1} and *samba*^{hkz2} mutations disrupt the early events of definitive hematopoiesis.

rumba^{hkz1} and *samba*^{hkz2} mutations compromise the HSPC maintenance in the CHT

We next investigated definitive HSPC development in both mutants. Previous studies have shown that zebrafish HSPCs initiate from the VDA region at ~28 hpf (Gering and Patient, 2005; Burns et al., 2005). The VDA-derived HSPCs subsequently migrate to the CHT at ~2 dpf and finally colonize the kidney by 5 dpf (Murayama et al., 2006; Jin et al., 2007). This developmental path of HSPCs can be followed by monitoring the expression of HSPC-associated genes such as *cmyb* (Murayama et al., 2006; Jin et al., 2007). Therefore, WISH was performed to examine *cmyb* expression in *rumba*$^{hkz1-/-}$ and *samba*$^{hkz2-/-}$ mutants at various developmental stages. We found that HSPCs were properly specified in both mutants as shown by intact *cmyb* expression in the VDA region at 30 hpf (Fig. 2A,A′,F,F′,K,K′,P,P′). Intriguingly, although HSPCs in *rumba*$^{hkz1-/-}$ could colonize the CHT at ~54 hpf (Fig. 2B,G,L,Q), their further development was compromised from 3 dpf onwards (Fig. 2C,H,M,R). In fact, whereas *cmyb* expression in siblings continued to increase in the CHT and appeared in the thymus and kidney by 4 dpf (Fig. 2D,I), this expression pattern was dramatically reduced in *rumba*$^{hkz1-/-}$ mutants (Fig. 2N,S). Similarly, in *samba*$^{hkz2-/-}$ mutants HSPCs were formed in the VDA and subsequently seeded the CHT as indicated by the enrichment of *cmyb* expression in the CHT up to 3 dpf (Fig. 2B′,C′,G′,H′,L′,M′,Q′,R′). However, *samba*$^{hkz2-/-}$ mutants started to show obvious decreased expression of *cmyb* in the CHT at ~4 dpf (Fig. 2D′,I′,N′,S′). By 5 dpf, *cmyb* expression was almost undetectable in the CHT, thymus and kidney of both *rumba*$^{hkz1-/-}$ and *samba*$^{hkz2-/-}$ mutants (Fig. 2E,E′,J,J′,O,O′,T,T′). A similar result was obtained by analyzing the *rumba*^{hkz1}/Tg(*cd41*:eGFP) and *samba*^{hkz2}/Tg(*cd41*:eGFP) lines carrying the *cd41*:eGFP transgene (see Fig. S2 in the supplementary material). The Tg(*cd41*:eGFP) transgenic line was recently shown to label definitive hematopoietic precursors, including HSPCs, in zebrafish (Kissa et al., 2008). As expected, large clusters of GFP-positive cells were found in the 5 dpf wild-type siblings CHT (see Fig. S2A,B in the supplementary material), whereas these hematopoietic precursors were reduced in both *rumba*$^{hkz1-/-}$/Tg(*cd41*:eGFP) and *samba*$^{hkz2-/-}$/Tg(*cd41*:eGFP) (see Fig. S2C-F in the supplementary material). These results show that both *rumba*^{hkz1} and *samba*^{hkz2} mutations do not affect HSPC initiation in the VDA and their subsequent mobilization to the CHT, but rather disrupt their maintenance and further development in the CHT. In particular, mutation of *rumba* compromised HSPC development as early as 3 dpf, soon after they colonize the CHT, whereas HSPCs in *samba*^{hkz2} mutants appeared to be compromised when they underwent further expansion in the CHT at ~4 dpf.

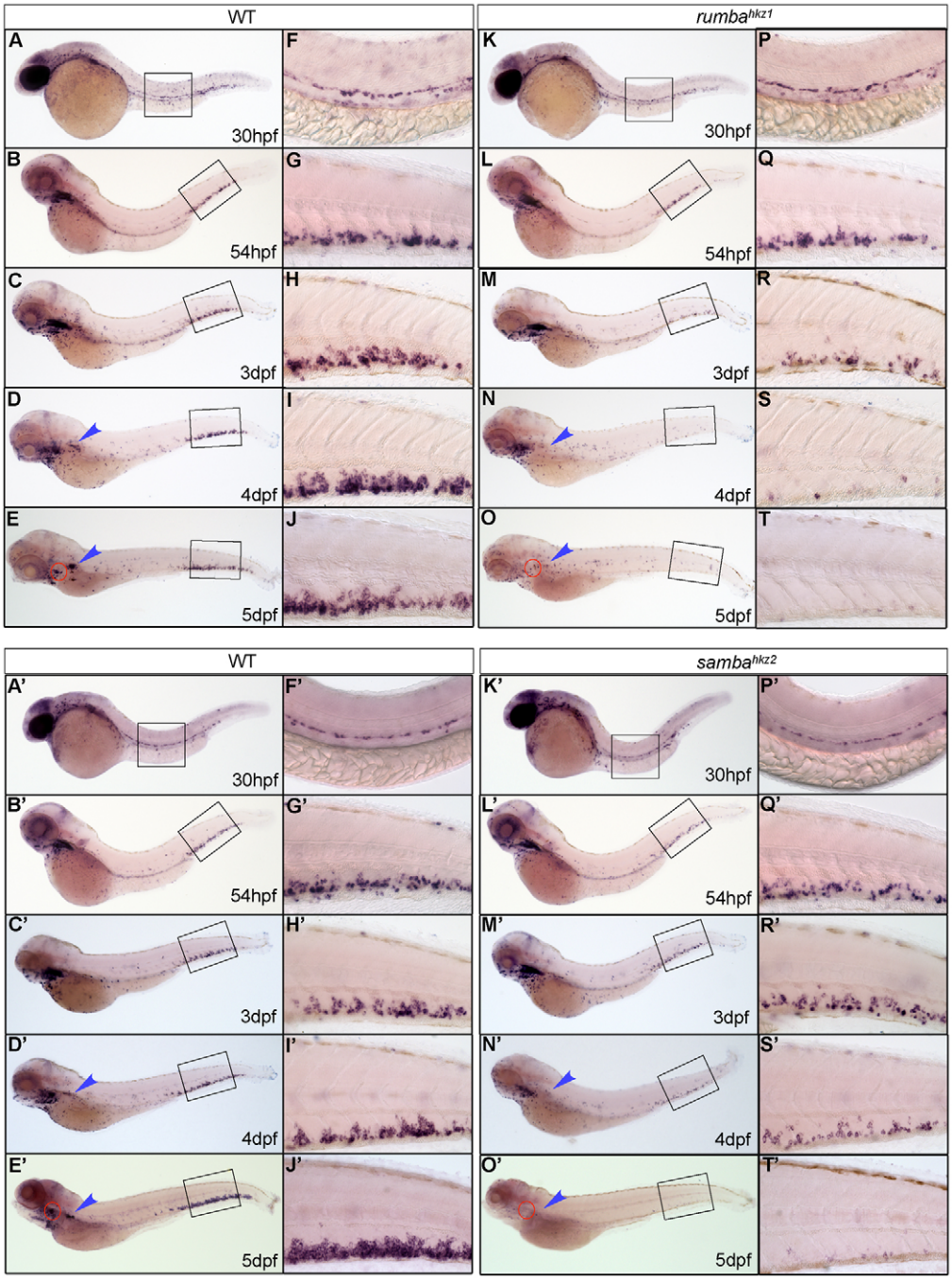

Fig. 2. Definitive HSPCs are not sustained in the CHT of *rumba*^{hkz1} and *samba*^{hkz2} mutants. (**A-T′**) WISH of *c-myb* in 30 hpf, 54 hpf, 3 dpf, 4 dpf and 5 dpf wild-type (WT) zebrafish siblings (A-E′) and *rumba*$^{hkz1-/-}$ (K-O), and *samba*$^{hkz2-/-}$ mutants (K′-O′). The right-hand columns (F-J′,P-T′) represent the 20× magnification of the boxed regions in the left-hand columns (A-E′,K-O′). The red circles and the blue arrowheads show the position of the thymus and kidney, respectively.

To define the cellular defects of the hematopoietic phenotype in these two mutants, we first monitored the cell death of HSPCs in *rumba*^{hkz1} and *samba*^{hkz2} mutants using Acridine Orange (AO) staining and the TUNEL assay. Both showed that there was either no significant increase or only a slight increase of apoptotic HSPCs in the CHT of both mutant embryos from 3 dpf to 5 dpf (see Fig. S3 in the supplementary material; data not shown). This result does not explain the drastic reduction of the hematopoietic cell phenotype in the CHT of both mutants. We therefore checked the HSPC proliferation status of both mutants. Anti-phospho-histone 3 (pH3) staining (Hendzel et al., 1997) revealed a block of HSPC proliferation in the CHT of *samba*$^{hkz2-/-}$ embryos at 4 dpf (Fig. 3). In siblings, double staining of *cmyb* and pH3 showed that only a small number of *cmyb*-expressing cells in the CHT was also pH3-positive and, thus, these cells were actually mitotic cells in the M phase (Fig. 3A-D). By contrast, although *cmyb* expression in the CHT was already decreased in *samba*$^{hkz2-/-}$ mutant embryos at 4 dpf, there was a significant increase of pH3-positive cells in the residual *cmyb*-expressing cells (Fig. 3E-H). This result strongly suggests that a large portion of the CHT-restricted hematopoietic cells, including HSPCs, in *samba*^{hkz2} mutants are blocked in the M phase during cell cycle progression so that their expansion and further differentiation are compromised, resulting in a loss of major definitive lineages. Living cell cycle analysis by Hoechst 33342 staining confirmed our speculation: the percentage of hematopoietic precursors (marked by *cd41*-GFP^{+} positive cells) in the G2/M stages (29.7%) was three times greater than in their siblings (8.9%; see Fig. S4A,B in the supplementary material). By

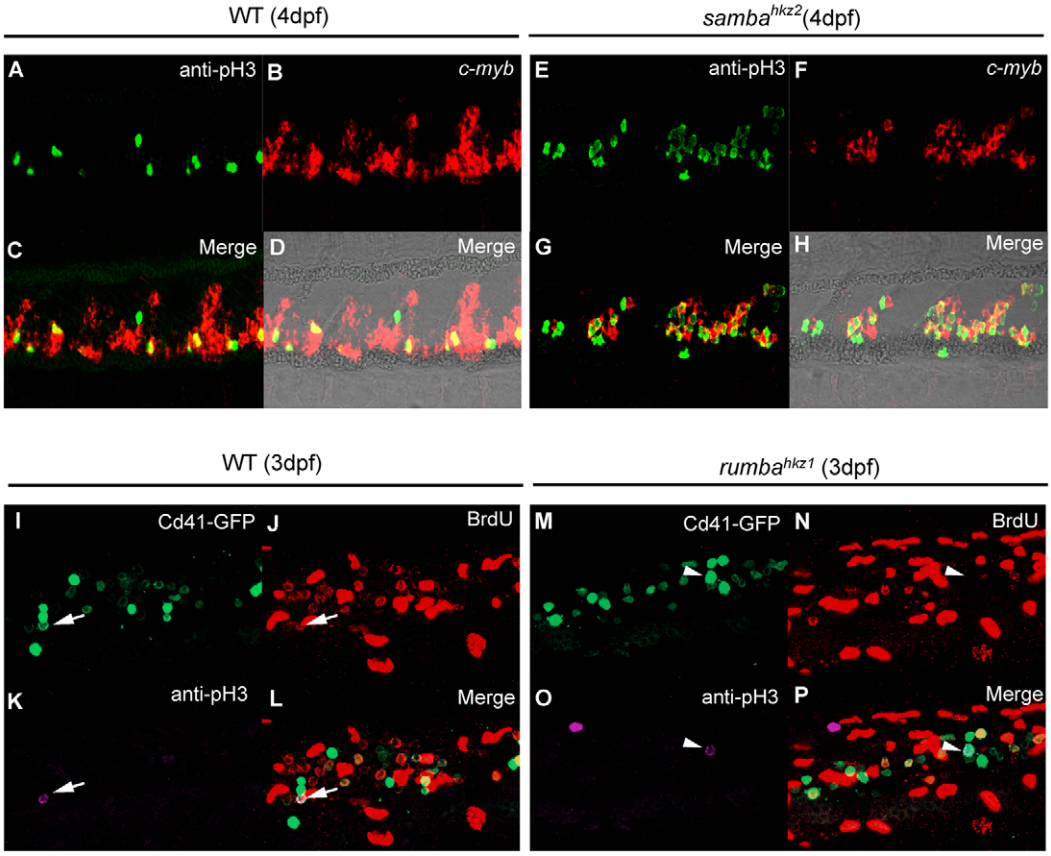

Fig. 3. *rumba*^{hkz1} and *samba*^{hkz2} mutations cause different cellular defects in definitive hematopoietic cells. (**A-H**) Double staining of *cmyb* RNA and phospho histone 3 (pH3) protein in the CHT of 4 dpf wild-type (WT) zebrafish siblings (A-D) and *samba*$^{hkz2-/-}$ mutants (E-H). D and H show bright-field images with fluorescent staining overlaid. (**I-P**) Triple staining of Cd41-GFP, BrdU and phospho histone 3 (pH3) of 3 dpf wild-type siblings (I-L) and *rumba*$^{hkz1-/-}$ mutants (M-P). Arrows indicate Cd41-GFP, BrdU and pH3 triple-positive cell and arrowheads indicate Cd41-GFP and pH3 double-positive but BrdU-negative cell.

contrast, in *rumba*$^{hkz1-/-}$ mutant embryos, no obvious increase of pH3-positive cells was found (data not shown). Living cell cycle analysis by Hoechst 33342 staining could not be applied to these embryos because it was difficult to differentiate *rumba*$^{hkz1-/-}$ mutant embryos from their siblings before 3 dpf, and hematopoietic cells in the 4 dpf *rumba*$^{hkz1-/-}$ mutant embryos were too few to perform cell cycle analysis. We therefore used BrdU labeling to examine the proliferation of HSPCs in *rumba*^{hkz1} mutants. *rumba*$^{hkz1-/-}$/Tg(*cd41*:eGFP) mutant embryos and their siblings were injected at 3 dpf with BrdU peritoneally and incubated for two hours. Co-staining of *cd41*-GFP and BrdU showed no obvious differences between *rumba*$^{hkz1-/-}$ embryos and siblings in the incorporation ratio of BrdU in HSPCs in the CHT region (Fig. 3I-P; see Fig. S4C in the supplementary material). However, we did find that the pH3 positive, BrdU negative HSPCs in the CHT region were significantly increased in *rumba*$^{hkz1-/-}$ mutant embryos (12 out of 33 cells) compared with their siblings (four out of 52 cells) (Table 1). The pH3 and BrdU double-positive HSPCs probably represent cells in M phase that had passed through S phase at least once, whereas pH3 positive but BrdU negative HSPCs are those in M phase that never entered the S phase during the incubation time. In other words, in siblings, most of the active proliferating HSPCs in the CHT had entered M phase by the end of the two hour incubation, as they are pH3 and BrdU double positive. In *rumba*$^{hkz1-/-}$ mutant embryos, however, a significant portion of HSPCs stayed in the M phase of the previous round of the cell cycle during the two hour interval as they were pH3 positive but BrdU negative, indicating delayed cell cycle progression of HSPCs in *rumba*$^{hkz1-/-}$ mutants. Taken together, these observations indicate that the failure to maintain the HSPC pool in *rumba*^{hkz1} and *samba*^{hkz2} mutants is caused by different cellular defects.

rumba gene encodes a nuclear zinc finger protein

A positional cloning approach was employed to identify the *rumba*^{hkz1} mutant gene. Bulk segregation analysis first mapped the *rumba* gene on linkage group 16 and fine mapping further placed the mutation within a 184 kb region between two simple sequence length polymorphism markers (SSLPs): O82105 and L25805 (Fig. 4A). This region is covered by four overlapping BACs, zC287M15, zC106K4, zC239E16 and zK67N17, and contains four predicted genes encoding the ETS domain transcriptional repressor PE1, a novel HMG protein, glycogen synthase kinase-3 alpha and a novel C2H2 zinc finger protein, respectively (Fig. 4A). Sequencing the coding region of these candidate genes revealed a point mutation in the gene encoding the novel C2H2 zinc finger protein, which contains 16 C2H2 zinc fingers with no other notable functional domains (Fig. 4F). This point mutation was a C-to-T

Table 1. Quantitative analysis of BrdU incorporation of Cd41$^+$ HSPCs in 3 dpf *rumba*^{hkz1} mutants and their siblings

Stage of BrdU labeling	Genotype	Cd41$^+$pH3$^+$ BrdU$^-$ cell number	Cd41$^+$pH3$^+$ BrdU$^+$ cell number	Percentage of Cd41$^+$pH3$^+$ BrdU$^-$ cells in all Cd41$^+$pH3$^+$ cells	Total number of embryos examined
3 dpf	*rumba*$^{hkz1-/-}$	12	21	36.4%	12
	sibling	4	48	7.7%	11

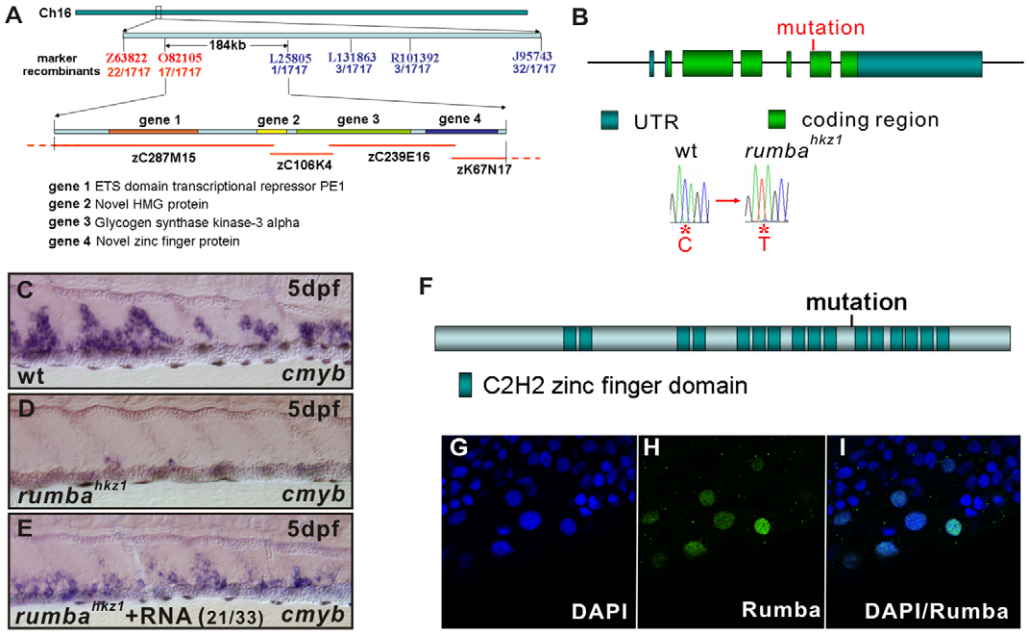

Fig. 4. *rumba* encodes a novel zinc finger protein. (**A**) The zebrafish rumba gene is mapped to a 184 kb region between two SSLP markers O82105 (17 recombinants in 1717 *rumba*$^{hkz1-/-}$ embryos) and L25805 (1 recombinant in 1717 *rumba*$^{hkz1-/-}$ embryos) in the LG16. This 184 kb region, covered by BAC zC287M15, zC106k4, zC239E16 and zK67N17, contains four predicted genes: the ETS domain transcriptional repressor PE1, a novel HMG protein, GSK-3α and the novel zinc finger protein. (**B**) The *rumba* gene consists of seven exons and a C-to-T substitution occurs in exon 6 in *rumba*^{hkz1} mutants. (**C-E**) WISH shows cmyb expression in the CHT of a 5 dpf a wild-type embryo (C), a *rumba*$^{hkz1-/-}$ mutant embryo (D) and a *rumba*$^{hkz1-/-}$ mutant embryo injected with synthesized wild-type *rumba* RNA (E). This phenotype is representative of 21 out of 33 mutant embryos observed, as indicated. (**F**) Protein sequence analysis predicts that Rumba consists of 16 C2H2 zinc-finger domains. (**G-I**) DAPI staining (G) and immunostaining with anti-Rumba antibody (H) reveals that Rumba is located in the nucleus as indicated by the colocalization of Rumba and DAPI (I).

transition that created a premature stop codon in exon 6, resulting in synthesis of a truncated protein lacking the C-terminal six zinc fingers (Fig. 4B,F). To confirm that the *rumba*$^{hkz1-/-}$ mutant phenotype was indeed caused by the nonsense mutation in this gene, we carried out a rescue experiment with in vitro transcribed mRNA. Injection of wild-type mRNA of the C2H2 zinc finger factor partially restored *cmyb* expression in *rumba*$^{hkz1-/-}$ mutant embryos (Fig. 4C-E; 21 rescued out of 33 injected mutants), whereas injection of the mutant mRNA failed to do so (data not shown). RT-PCR confirmed that the injected *rumba* cRNA was sustained until 4 dpf (see Fig. S5 in the supplementary material). Collectively, these data demonstrate that the gene encoding this C2H2 zinc finger protein is responsible for the *rumba*$^{hkz1-/-}$ mutant phenotype. As Rumba is predominantly localized in the nucleus (Fig. 4G-I), we speculate that Rumba could function as a transcriptional modulator.

samba^{hkz2} mutant phenotype is caused by a nonsense mutation in the zebrafish homolog of mammalian *HAUS3*

Using the positional cloning approach described in the previous section, the *samba*^{hkz2} mutation was mapped to a 300 kb region covered by three overlapping BACs on linkage group 7 (Fig. 5A). There are a total of eight genes predicted to be located in this region. Sequencing of the coding region of these candidate genes revealed a nonsense point mutation, a T-to-G transition creating a premature stop codon in the transcript, in gene *zgc153228* in the *samba*^{hkz2} mutant (Fig. 5B). Based on expressed sequence tag information and the RACE result, we obtained the full-length *zgc:153228* cDNA (*zgc153228*-β). Interestingly, a comparison of our cDNA sequence (*zgc:153228*-β) with another cDNA sequence from the NCBI database (*zgc:153228*-α) revealed a 48 bp (encoding 16 amino acids) difference in the coding region. This 48 bp sequence, which is part of exon 4 in *zgc:153228*-β, is spliced out in *zgc:153228*-α (Fig. 5C). RT-PCR also confirmed the existence of two forms of *zgc:153228* transcripts (data not shown).

To confirm that the *samba*^{hkz2} mutant phenotype was indeed caused by the nonsense mutation in *zgc:153228*, we performed a rescue experiment with in vitro synthesized *zgc:153228* mRNA. Injection of either form of wild-type *zgc:153228* mRNA into the *samba*$^{hkz2-/-}$ mutant embryos partially restored *cmyb* expression in the CHT (Fig. 5G-J) (α form: 10 rescued out of 38 injected mutants; β form: 18 rescued out of 55 injected mutants); whereas injection of the mutant mRNA failed to do so (data not shown). RT-PCR confirmed the presence of the injected *zgc:153228*-β RNA at 4 dpf (see Fig. S5 in the supplementary material). Based on the positional cloning data and rescue experiment result, we conclude that the nonsense mutation in *zgc:153228* gene does cause the *samba*^{hkz2} mutant phenotype. The predicted *zgc:153228* open reading frame encodes a 629 amino acid protein with two coiled-coil features. Protein sequence alignment and synteny analysis revealed that it is the homolog of the newly identified human augmin-like complex subunit 3 (HAUS3), which is crucial for mitotic spindle assembly, maintenance of centrosome integrity and mitotic progression in mammalian cell lines (Uehara et al., 2009; Lawo et al., 2009). We hereafter refer to the *samba* (*zgc:153228*) gene as *haus3*. Similar to mammalian HAUS3, immunohistochemical analysis of cos-7 cells transiently transfected with V5-tagged *haus3* cDNA constructs (*haus3*-α and *haus3*-β) revealed that Haus3 was exclusively localized in the cytoplasm

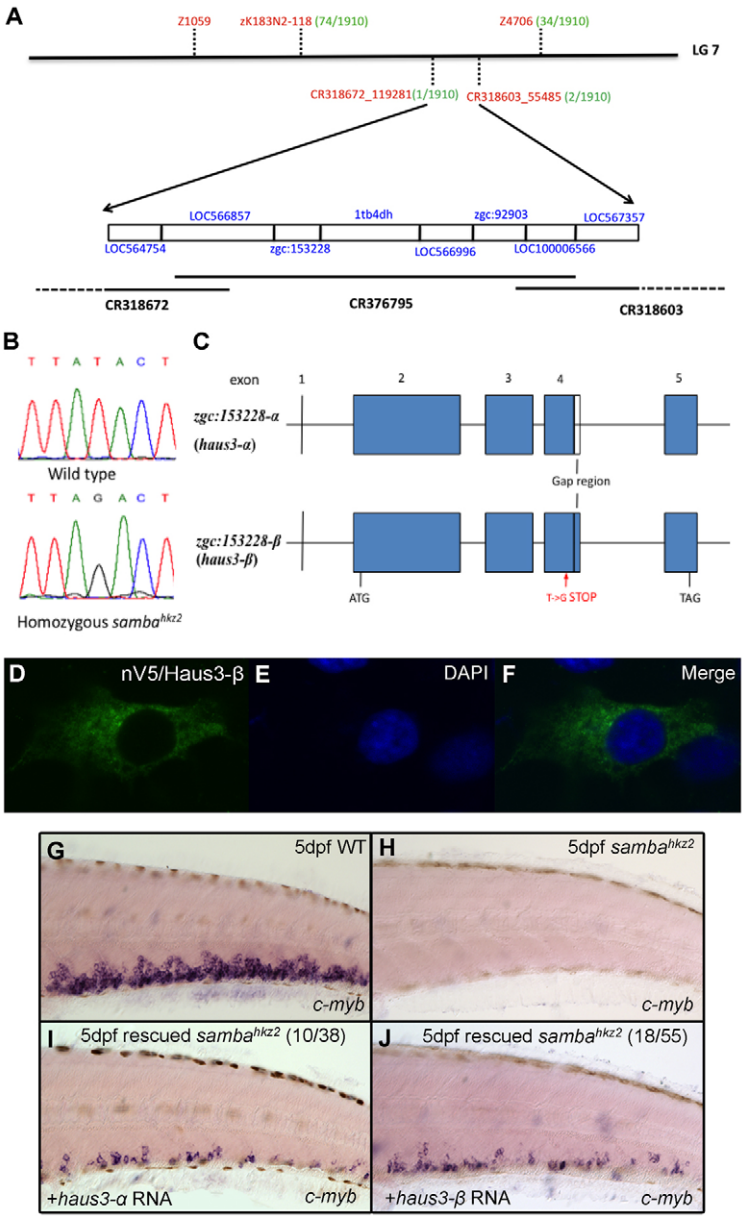

Fig. 5. The *samba*^{hkz2} mutation is mapped to the *haus3* gene in linkage group 7 of the zebrafish genome. (**A**) Positional cloning information. The *samba*^{hkz2} *mutation* is mapped to a three-overlapping-BAC region between markers CR318672_119281 and CR318603_55485 in LG7. This region contains eight candidate genes (blue). The simple sequence length polymorphism markers (SSLP) or single nucleotide polymorphism (SNP) markers used in mapping are labeled in red with their respective recombinants number (out of a total of 1910 homozygous *samba*^{hkz2} embryos) in green. (**B**) Sequencing results showing a nonsense mutation (a T-to-G transition) in *haus3* (*zgc:153228*) gene. (**C**) Gene structure of *haus3* (*zgc:153228*). Gap region indicates the absence of 48 bp in *haus3*-α (*zgc:153228*-α). (**D-F**) Immunohistochemical staining with the anti-V5 monoclonal antibody on pcDNA3.1/nV5-*haus3*-β-transfected cos-7 cells and DAPI staining of the same transfected cells. (**G-J**) In vitro synthesized full-length *haus3* RNA rescues the mutant phenotype. WISH of *cmyb* expression in wild type (G), uninjected *samba*$^{hkz2-/-}$ mutant control (H) and *samba*$^{hkz2-/-}$ mutant embryos injected with either wild-type *haus3*-α (I) or *haus3*-β RNA (J). The phenotype seen in I and J is representative of 10 out of 38 and 18 out of 55 mutant embryos observed, as indicated.

(Fig. 5D-F; data not shown). Although two splicing forms of *haus3* transcripts exist during embryonic development, Haus3-α and Haus3-β proteins show the same localization patterns and can rescue the mutant hematopoietic phenotype to similar extent. Therefore, they seem to be functionally equivalent during hematopoiesis.

Rumba and Haus3 are cell autonomously required for maintaining the HSPC pool in the CHT

In order to address how loss of the *rumba* and *haus3* genes causes hematopoietic defects, we first examined the temporal and spatial expression pattern of these two genes by WISH. Both genes exhibited a widespread expression in the embryonic body rather than being specific to the hematopoietic tissues (see Fig. S6 in the supplementary material). This raised the question of whether the hematopoietic phenotype observed in *rumba*$^{hkz1-/-}$ and *samba*$^{hkz2-/-}$ mutants was caused by a cell-autonomous or non-cell-autonomous effect. To clarify this issue, a cell transplantation experiment was performed in which donor cells derived from 3 hpf wild-type Tg(*cd41*:eGFP) embryos were transplanted into either the same stage *rumba*$^{hkz1-/-}$ and *samba*$^{hkz2-/-}$ mutants or their siblings. We reasoned that if the hematopoietic phenotype in both mutants was caused by a cell-autonomous effect, the contribution of transplanted wild-type donor cells to the HSPCs in the CHT in both mutant hosts would be comparable to that in siblings. Indeed, wild-type donor GFP positive cells were detected in the CHT region of both *rumba*$^{hkz1-/-}$ and *samba*$^{hkz2-/-}$ hosts, and the contribution ratios were similar to that observed in sibling hosts (Table 2). Notably, those GFP-positive donor cells could form large colonies in the CHT of both mutants and many of them were able to differentiate into αE1-globin-positive erythroid precursors (Fig. 6), implying that the *rumba*$^{hkz1-/-}$ and *samba*$^{hkz2-/-}$ mutant embryos can not only accommodate wild-type cells but also support their proliferation and differentiation. This result suggests that both Rumba and Haus3 act cell autonomously. To further confirm this, we performed reciprocal transplantation in which donor cells derived from 3 hpf *rumba*$^{hkz1-/-}$ and *samba*$^{hkz2-/-}$ mutants in a Tg(*cd41*:eGFP) background were transplanted into wild-type hosts.

Table 2. Summary of transplantation results

Donor	Host	Total number of host embryos	Number of host embryos with Cd41-GFP$^+$ donor-derived cells in the CHT		
			With over 20 Cd41-GFP$^+$ cells	With 1-19 Cd41-GFP$^+$ cells	Total
wild type	*rumba*$^{hkz1-/-}$	322	6	1	7
wild type	sibling of *rumba*$^{hkz1-/-}$		21	7	28
wild type	*samba*$^{hkz2-/-}$	198	4	4	8
wild type	sibling of *samba*$^{hkz2-/-}$		13	7	20
rumba$^{hkz1-/-}$	wild type	304	0	2	2
sibling of *rumba*$^{hkz1-/-}$	wild type		14	10	24
samba$^{hkz2-/-}$	wild type	363	0	1	1
sibling of *samba*$^{hkz2-/-}$	wild type		6	8	14

CBT, caudal hematopoietic tissue.

As expected, we found that many fewer mutant donor cells were detected in host CHT compared with sibling donor cells (Table 2). Collectively, these data demonstrate that both Rumba and Haus3 act in a cell-autonomous manner in maintaining the HSPC pool in the CHT during fetal hematopoiesis.

DISCUSSION

In this study, we report the isolation of two zebrafish mutant lines *rumba*^{hkz1} and *samba*^{hkz2} from our genetic screen aiming to identify novel factors regulating definitive hematopoiesis and HSPC development. Characterization results suggest that the early-forming tissues are largely normal in both mutants and they can both produce primitive hematopoiesis. It has been reported that there is a separate population of committed erythromyeloid progenitors (EMPs) initiating definitive hematopoiesis independent of HSPCs (Bertrand et al., 2007) and this population seems to be unaffected in these two mutants as determined by checking a few erythroid and myeloid marker genes at ~33 hpf (data not shown). We found that although definitive HSPCs were initially specified in the VDA region and could subsequently seed the CHT, their further development was severely impaired in *rumba*^{hkz1} and *samba*^{hkz2} mutants. In particular, loss of *rumba* affected HSPC maintenance as early as they colonize the CHT, whereas HSPCs in *samba*^{hkz2} mutants were affected in the late stage of HSPC expansion in the CHT. Bertrand et al. have reported that HSPCs can also migrate to the kidney along the renal tube

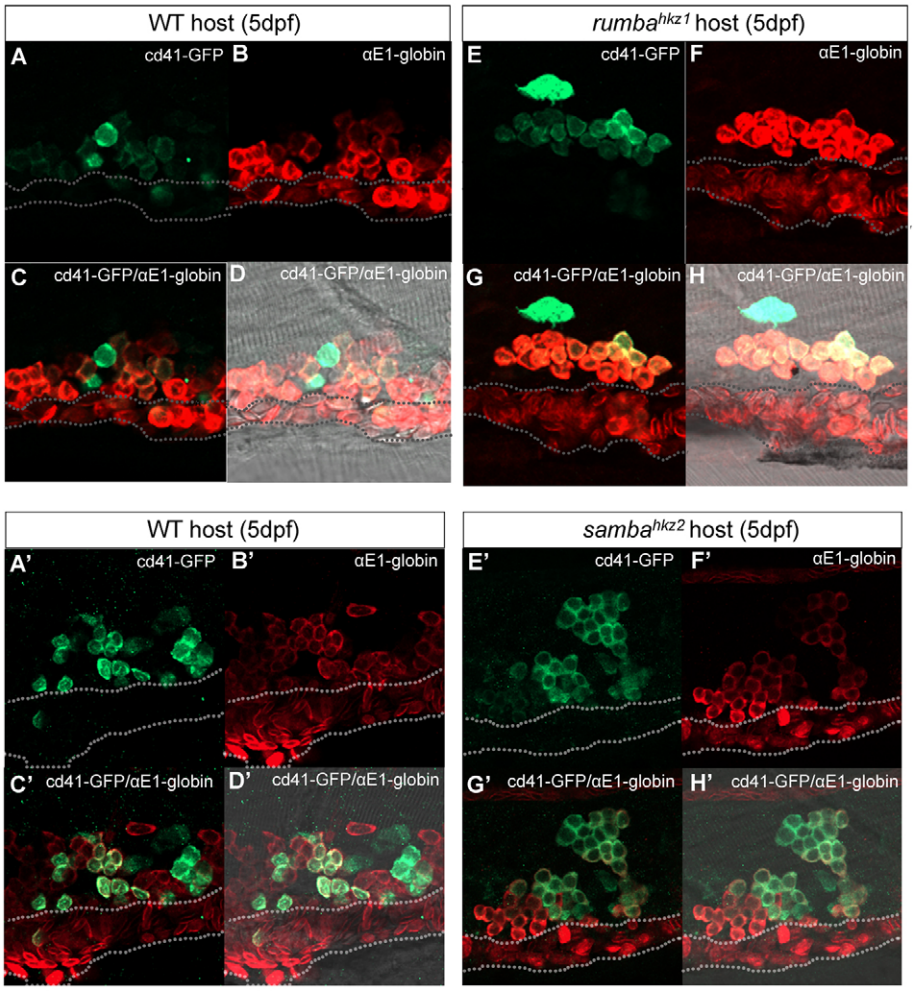

Fig. 6. Rumba and Haus3 are cell autonomously required for maintaining HSPCs in the CHT. (**A-H'**) Confocal images of transplantation results in wild-type (WT) zebrafish sibling hosts (A-D'), *rumba*$^{hkz1-/-}$ mutant hosts (E-H), and *samba*$^{hkz2-/-}$ mutant hosts (E'-H'). Anti-GFP staining (A,A',E,E') and anti-αE1-globin staining (B,B',F,F') in the host CHT region are merged in C, C', G and G', as indicated and superimposed with their respective bright field views in D, D', H and H'. Dotted lines indicate the position of the caudal vein.

(Bertrand et al., 2008). However, the nature of this HSPC population remains undefined. Nonetheless, we speculate that *rumba* and *haus3* are also required for the development of this HSPC population, presumably in a manner similar to HSPCs in the CHT, because almost no, or very low levels of, hematopoietic marker was detected in the kidney of both mutants (Fig. 1). Further study with markers that specifically mark this HSPC population will help to clarify this issue. Our findings highlight the divergence of the molecular machinery governing the initiation and maintenance of HSPCs. This divergence seems to be conserved among vertebrates. For example, *Tal1* and *Runx1* are found to be necessary for the initiation, but dispensable for the maintenance of, hematopoietic stem cells in mice (Mikkola et al., 2003; Ichikawa et al., 2004). By contrast, *Sox17* is essential for the maintenance of fetal hematopoiesis, but it is dispensable for the initiation of definitive hematopoiesis and adult hematopoiesis (Kim et al., 2007).

Our study shows that cell cycle defects are the primary defects that contribute to the hematopoietic phenotype in *rumba*^{hkz1} and *samba*^{hkz2} mutants. The absence of both HSPCs and differentiated blood cells in the CHT region in both mutants by 5 dpf indicates that the abnormal hematopoietic cells eventually die. However, TUNEL staining reveals only a subtle increase in the number of dying cells in the CHT region in both mutants (see Fig. S3 in the supplementary material). The most likely explanations for this result are: (1) HSPCs were not properly expanded in both mutants, thus the total cell number is less than that in wild type from 3 dpf onwards; (2) Those defective hematopoietic cells in the CHT are possibly cleared in an unsynchronized and gradual manner. In summary, we believe that cell cycle defects shown in both mutants represent the main cellular defects and that they eventually cause secondary consequences such as clearance of abnormal cells, presumably by apoptosis.

Although *rumba*^{hkz1} and *samba*^{hkz2} mutants have a similar hematopoietic phenotype, our current evidence indicates that these two genes are involved in different pathways. First, the appearance of hematopoietic defects was earlier in *rumba*^{hkz1} than in *samba*^{hkz2} mutants. Furthermore, the cell cycle arrest phenotype that occurred in *samba*^{hkz2} mutants was not found in *rumba*^{hkz1}; instead, *rumba*^{hkz1} demonstrated a cell cycle delay defect. No discernible difference of *rumba* expression was detected between *samba*^{hkz2} mutants and their siblings (data not shown). Moreover, neither Rumba nor Haus3 can rescue each other's phenotype (data not shown). Thus, Rumba and Haus3 probably function independently in the regulation of HSPC development.

Protein sequence analysis revealed that the zinc finger protein 585B (NM 152279) is the most similar human protein to Rumba. However, 585B also shares a high degree of homology with several other zebrafish zinc finger proteins owing to multiple C2H2 zinc finger domains (data not shown). It is unclear whether 585B is the mammalian counterpart of zebrafish Rumba and further functional assays should be carried out in zebrafish or a mammalian system to clarify this issue. By contrast, protein sequence alignment and synteny analysis showed that the zebrafish Samba protein is homologous to one of the subunits of human augmin complex HAUS3, which is crucial for mitotic spindle assembly, maintenance of centrosome integrity and mitotic progression in Hela cells (Uehara et al., 2009; Lawo et al., 2009). We showed that the failure of developing fetal hematopoiesis in the *samba*^{hkz2} mutant CHT was similarly due to the arrest of HSPCs at the M phase during cell cycle progression as shown by both pH3 staining and FACS analysis. Thus, our findings not only support these human cell line studies but, more importantly, provide genetic evidence for the physiological significance of the human augmin complex in the regulation of HSPC development in vertebrates. The functional similarity of zebrafish Haus3 and human HAUS3 is also supported by the high degree of conservation in their amino acid sequence and protein structure: zebrafish Haus3 has two coiled-coil motifs (amino acids ~108-135 and ~500-527) and human HAUS3 contains several coiled-coil features. Coiled-coil is a typical hypersecondary structure formed by two or more α-helices, and short coiled-coil domains usually mediate specific protein-protein interactions (Rose and Meier, 2004). We speculate that such conserved features might be responsible for the physical interaction with other subunits in the HAUS complex or γ-tubulin ring complex (Uehara et al., 2009).

The transplantation assay demonstrates that both *rumba* and *haus3* act cell autonomously in maintaining the HSPC pool in the CHT. However, a non-cell-autonomous effect of these two genes cannot be excluded at this stage. Given the fact that all the αE1-positive hematopoietic colonies found in the transplanted host mutant CHT were derived exclusively from donor cells as shown by the fact that they were GFP positive (Fig. 6), we speculate that a non-cell-autonomous effect, if it exists, would be minimal. Of note, in the transplantation assay, we also found that transplanted wild-type donor cells appeared to form large colonies in the CHT region of both mutants, whereas in control siblings transplanted cells tended to spread as small clusters. This phenomenon suggests that the CHT niche in the mutants can impose a compensation feedback loop when healthy donors successfully dock into it.

The identification of *rumba* and *haus3* genes as crucial regulators of HSPC development demonstrates the power of the zebrafish system to uncover novel factors involved in hematopoiesis. Besides *rumba*^{hkz1} and *samba*^{hkz2}, a collection of definitive hematopoiesis defective zebrafish mutants were recovered from our genetic screen. With the cloning and characterization of those mutants, we believe that a great deal will be learned to fill the gaps in our current understanding of HSPC development.

Acknowledgements
We thank Dr Robert I. Handin (Brigham & Women's Hospital, USA) for providing Tg(*cd41*:eGFP) fish. We also thank Bernard Teo and Augustine Chong for excellent technical assistance and Claudia Seger for providing the TUNEL protocol. This work was supported by the Area of Excellence Scheme established under the University Grants Committee of the HKSAR (Grant No.: AoE/B-15/01), by the GRF grant from the Research Grants Council of the HKSAR (Grant No.: 662808) and by the National Natural Science Foundation of China (Grant No.: 30828020).

Competing interests statement
The authors declare no competing financial interests.

Supplementary material
Supplementary material for this article is available at
http://dev.biologists.org/lookup/suppl/doi:10.1242/dev.054536/-/DC1

References
Amatruda, J. F. and Zon, L. I. (1999). Dissecting hematopoiesis and disease using the zebrafish. *Dev. Biol.* **216**, 1-15.
Bahary, N. and Zon, L. I. (1998). Use of the zebrafish (Danio rerio) to define hematopoiesis. *Stem Cells* **16**, 89-98.
Bahary, N., Davidson, A., Ransom, D., Shepard, J., Stern, H., Trede, N., Zhou, Y., Barut, B. and Zon, L. I. (2004). The Zon laboratory guide to positional cloning in zebrafish. *Methods Cell Biol.* **77**, 305-329.
Bennett, C. M., Kanki, J. P., Rhodes, J., Liu, T. X., Paw, B. H., Kieran, M. W., Langenau, D. M., Delahaye-Brown, A., Zon, L. I., Fleming, M. D. et al. (2001). Myelopoiesis in the zebrafish, Danio rerio. *Blood* **98**, 643-651.
Bertrand, J. Y., Kim, A. D., Violette, E. P., Stachura, D. L., Cisson, J. L., Traver, D. (2007). Definitive hematopoiesis initiates through a committed

erythromyeloid progenitor in the zebrafish embryo. *Development* **134**, 4147-4156.
Bertrand, J. Y., Kim, A. D., Teng, S. and Traver, D. (2008). CD41+ cmyb+ precursors colonize the zebrafish pronephros by a novel migration route to initiate adult hematopoiesis. *Development* **135**, 1853-1862.
Brownlie, A., Hersey, C., Oates, A. C., Paw, B. H., Falick, A. M., Witkowska, H. E., Flint, J., Higgs, D., Jessen, J., Bahary, N. et al. (2003). Characterization of embryonic globin genes of the zebrafish. *Dev. Biol.* **255**, 48-61.
Burns, C. E., DeBlasio, T., Zhou, Y., Zhang, J., Zon, L. I. and Nimer, S. D. (2002). Isolation and characterization of runxa and runxb, zebrafish members of the runt family of transcriptional regulators. *Exp. Hematol.* **30**, 1381-1389.
Burns, C. E., Traver, D., Mayhall, E., Shepard, J. L. and Zon, L. I. (2005). Hematopoietic stem cell fate is established by the Notch-Runx pathway. *Genes Dev.* **19**, 2331-2342.
Burns, C. E., Galloway, J. L., Smith, A. C., Keefe, M. D., Cashman, T. J., Paik, E. J., Mayhall, E. A., Amsterdam, A. H. and Zon, L. I. (2009). A genetic screen in zebrafish defines a hierarchical network of pathways required for hematopoietic stem cell emergence. *Blood* **113**, 5776-5782.
Cheshier, S. H., Morrison, S. J., Liao, X. and Weissman, I. L. (1999). In vivo proliferation and cell cycle kinetics of long-term self-renewing hematopoietic stem cells. *Proc. Natl. Acad. Sci. USA* **96**, 3120-3125.
Cumano, A., Dieterlen-Lievre, F. and Godin, I. (1996). Lymphoid potential, probed before circulation in mouse, is restricted to caudal intraembryonic splanchnopleura. *Cell* **86**, 907-916.
Davidson, A. J. and Zon, L. I. (2004). The 'definitive' (and 'primitive') guide to zebrafish hematopoiesis. *Oncogene* **23**, 7233-7246.
de Jong, J. L. and Zon, L. I. (2005). Use of the zebrafish system to study primitive and definitive hematopoiesis. *Annu. Rev. Genet.* **39**, 481-501.
Furutani-Seiki, M., Jiang, Y. J., Brand, M., Heisenberg, C. P., Houart, C., Beuchle, D., van Eeden, F. J., Granato, M., Haffter, P., Hammerschmidt, M. et al. (1996). Neural degeneration mutants in the zebrafish, Danio rerio. *Development* **123**, 229-239.
Gekas, C., Dieterlen-Lievre, F., Orkin, S. H. and Mikkola, H. K. (2005). The placenta is a niche for hematopoietic stem cells. *Dev. Cell* **8**, 365-375.
Gering, M. and Patient, R. (2005). Hedgehog signaling is required for adult blood stem cell formation in zebrafish embryos. *Dev. Cell* **8**, 389-400.
Goessling, W., North, T. E., Loewer, S., Lord, A. M., Lee, S., Stoick-Cooper, C. L., Weidinger, G., Puder, M., Daley, G. Q., Moon, R. T. et al. (2009). Genetic interaction of PGE2 and Wnt signaling regulates developmental specification of stem cells and regeneration. *Cell* **136**, 1136-1147.
Hendzel, M. J., Wei, Y., Mancini, M. A., Van Hooser, A., Ranalli, T., Brinkley, B. R., Bazett-Jones, D. P. and Allis, C. D. (1997). Mitosis-specific phosphorylation of histone H3 initiates primarily within pericentromeric heterochromatin during G2 and spreads in an ordered fashion coincident with mitotic chromosome condensation. *Chromosoma* **106**, 348-360.
Ichikawa, M., Asai, T., Saito, T., Seo, S., Yamazaki, I., Yamagata, T., Mitani, K., Chiba, S., Kurokawa, M. and Hirai, H. (2004). AML-1 is required for megakaryocytic maturation and lymphocytic differentiation, but not for maintenance of hematopoietic stem cells in adult hematopoiesis. *Nat. Med.* **10**, 299-304.
Jin, H., Xu, J., Qian, F., Du, L., Tan, C. Y., Lin, Z., Peng, J. and Wen, Z. L. (2006). The 5′ zebrafish scl promoter targets transcription to the brain, spinal cord, and hematopoietic and endothelial progenitors. *Dev. Dyn.* **235**, 60-67.
Jin, H., Xu, J. and Wen, Z. L. (2007). Migratory path of definitive hematopoietic stem/progenitor cells during zebrafish development. *Blood* **109**, 5208-5214.
Jin, H., Sood, R., Xu, J., Zhen, F., English, M. A., Liu, P. P. and Wen, Z. L. (2009). Definitive hematopoietic stem/progenitor cells manifest distinct differentiation output in the zebrafish VDA and PBI. *Development* **136**, 647-654.
Kalev-Zylinska, M. L., Horsfield, J. A., Flores, M. V., Postlethwait, J. H., Vitas, M. R., Baas, A. M., Crosier, P. S. and Crosier, K. E. (2002). Runx1 is required for zebrafish blood and vessel development and expression of a human RUNX1-CBF2T1 transgene advances a model for studies of leukemogenesis. *Development* **129**, 2015-2030.
Kim, I., Saunders, T. L. and Morrison, S. J. (2007). Sox17 dependence distinguishes the transcriptional regulation of fetal from adult hematopoietic stem cells. *Cell* **130**, 470-483.
Kissa, K., Murayama, E., Zapata, A., Cortes, A., Perret, E., Machu, C. and Herbomel, P. (2008). Live imaging of emerging hematopoietic stem cells and early thymus colonization. *Blood* **111**, 1147-1156.
Lawo, S., Bashkurov, M., Mullin, M., Ferreria, M. G., Kittler, R., Habermann, B., Tagliaferro, A., Poser, I., Hutchins, J. R., Hegemann, B. et al. (2009). HAUS, the 8-subunit human Augmin complex, regulates centrosome and spindle integrity. *Curr. Biol.* **19**, 816-826.
Lieschke, G. J. and Currie, P. D. (2007). Animal models of human disease: zebrafish swim into view. *Nat. Rev. Genet.* **8**, 353-367.
Lin, H. F., Traver, D., Zhu, H., Dooley, K., Paw, B. H., Zon, L. I. and Handin, R. I. (2005). Analysis of thrombocyte development in CD41-GFP transgenic zebrafish. *Blood* **106**, 3803-3810.
Liu, Y., Du, L., Osato, M., Teo, E. H., Qian, F., Jin, H., Zhen, F., Xu, J., Guo, L., Huang, H. et al. (2007). The zebrafish udu gene encodes a novel nuclear factor and is essential for primitive erythroid cell development. *Blood* **110**, 99-106.
Medvinsky, A. and Dzierzak, E. (1996). Definitive hematopoiesis is autonomously initiated by the AGM region. *Cell* **86**, 897-906.
Mikkola, H. K. and Orkin, S. H. (2006). The journey of developing hematopoietic stem cells. *Development* **133**, 3733-3744.
Mikkola, H. K., Klintman, J., Yang, H., Hock, H., Schlaeger, T. M., Fujiwara, Y. and Orkin, S. H. (2003). Haematopoietic stem cells retain long-term repopulating activity and multipotency in the absence of stem-cell leukaemia SCL/tal-1 gene. *Nature* **421**, 547-551.
Moore, M. S. A. and Metcalf, D. (1970). Ontogeny of the haemopoietic system: yolk sac origin of in vivo and in vitro colony forming cells in the developing mouse embryo. *Br. J. Haemat.* **18**, 279-296.
Morrison, S. J., Uchida, N. and Weissman, I. L. (1995). The biology of hematopoietic stem cells. *Annu. Rev. Cell Dev. Biol.* **11**, 35-71.
Muller, A. M., Medvinsky, A., Strouboulis, J., Grosveld, F. and Dzierzak, E. (1994). Development of hematopoietic stem cell activity in the mouse embryo. *Immunity* **1**, 291-301.
Mullins, M. C., Hammerschmidt, M., Haffter, P. and Nüsslein-Volhard, C. (1994). Large-scale mutagenesis in the zebrafish: in search of genes controlling development in a vertebrate. *Curr. Biol.* **4**, 189-202.
Murayama, E., Kissa, K., Zapata, A., Mordelet, E., Briolat, V., Lin, H. F., Handin, R. I. and Herbomel, P. (2006). Tracing hematopoietic precursor migration to successive hematopoietic organs during zebrafish development. *Immunity* **25**, 963-975.
North, T. E., Goessling, W., Walkley, C. R., Lengerke, C., Kopani, K. R., Lord, A. M., Weber, G. J., Bowman, T. V., Jang, I. H., Grosser, T. et al. (2007). Prostaglandin E2 regulates vertebrate haematopoietic stem cell homeostasis. *Nature* **447**, 1007-1011.
North, T. E., Goessling, W., Peeters, M., Li, P., Ceol, C., Lord, A. M., Weber, G. J., Harris, J., Cutting, C. C., Huang, P. et al. (2009). Hematopoietic stem cell development is dependent on blood flow. *Cell* **137**, 736-748.
Ottersbach, K. and Dzierzak, E. (2005). The murine placenta contains hematopoietic stem cells within the vascular labyrinth region. *Dev. Cell* **8**, 377-387.
Rose, A. and Meier, I. (2004). Scaffolds, levers, rods and springs: diverse cellular functions of long coiled-coil proteins. *Cell. Mol. Life Sci.* **61**, 1996-2009.
Samokhvalov, I. M., Samokhvalova, N. I. and Nishikawa, S. (2007). Cell tracing shows the contribution of the yolk sac to adult haematopoiesis. *Nature* **446**, 1056-1061.
Solnica-Krezel, L., Schier, A. F. and Driever, W. (1994). Efficient recovery of ENU-induced mutations from the zebrafish germline. *Genetics* **136**, 1401-1420.
Thompson, M. A., Ransom, D. G., Pratt, S. J., MacLennan, H., Kieran, M. W., Detrich, H. W., III, Vail, B., Huber, T. L., Paw, B., Brownlie, A. J. et al. (1998). The cloche and spadetail genes differentially affect hematopoiesis and vasculogenesis. *Dev. Biol.* **197**, 248-269.
Traver, D., Paw, B. H., Poss, K. D., Penberthy, W. T., Lin, S. and Zon, L. I. (2003). Transplantation and in vivo imaging of multilineage engraftment in zebrafish bloodless mutants. *Nat. Immunol.* **4**, 1238-1246.
Trede, N. S., Ota, T., Kawasaki, H., Paw, B. H., Katz, T., Demarest, B., Hutchinson, S., Zhou, Y., Hersey, C., Zapata, A. et al. (2008). Zebrafish mutants with disrupted early T-cell and thymus development identified in early pressure screen. *Dev. Dyn.* **237**, 2575-2584.
Uehara, R., Nozawa, R. S., Tomioka, A., Petry, S., Vale, R. D., Obuse, C. and Goshima, G. (2009). The augmin complex plays a critical role in spindle microtubule generation for mitotic progression and cytokinesis in human cells. *Proc. Natl. Acad. Sci. USA* **106**, 6998-7003.
Wallace, K. N., Akhter, S., Smith, E. M., Lorent, K. and Pack, M. (2005). Intestinal growth and differentiation in zebrafish. *Mech. Dev.* **122**, 157-173.
Weissman, I. L. (2000). Stem cells: units of development, units of regeneration, and units in evolution. *Cell* **100**, 157-168.
Westerfield, M. (2000). *The Zebrafish Book. A Guide for the Laboratory Use of Zebrafish (Danio rerio)*. Eugene, OR: University of Oregon Press.
Willett, C. E., Cherry, J. J. and Steiner, L. A. (1997). Characterization and expression of the recombination activating genes (rag1 and rag2) of zebrafish. *Immunogenetics* **45**, 394-404.
Willett, C. E., Kawasaki, H., Amemiya, C. T., Lin, S. and Steiner, L. A. (2001). Ikaros expression as a marker for lymphoid progenitors during zebrafish development. *Dev. Dyn.* **222**, 694-698.
Zhang, X. Y. and Rodaway, A. R. F. (2007). SCL-GFP transgenic zebrafish: In vivo imaging of blood and endothelial development and identification of the initial site of definitive hematopoiesis. *Dev. Biol.* **307**, 179-194.